Sound Waves and the Absence of Galilean Invariance in Flocks

Yuhai Tu
IBM T. J. Watson Research Center, P.O. Box 218, Yorktown Heights, New York 10598

John Toner and Markus Ulm
Department of Physics, University of Oregon, Eugene, Oregon 97403-1274

(Received 22 October 1997)

We study a model of flocking for a very large system ($N = 320\,000$) numerically. We find that in the long wavelength, long time limit, the fluctuations of the velocity and density fields are carried by propagating sound modes, whose dispersion and damping agree quantitatively with the predictions of our previous work using a continuum equation. We find that the sound velocity is anisotropic and characterized by its speed c for propagation perpendicular to the mean velocity $\langle\vec{v}\rangle$, $\langle\vec{v}\rangle$ itself, and a third velocity $\lambda\langle\vec{v}\rangle$, arising explicitly from the lack of Galilean invariance in flocks. [S0031-9007(98)06186-9]

PACS numbers: 87.10.+e, 05.60.+w, 64.60.Cn

The dynamics of "flocking" behavior of living things, such as birds, fish, wildebeest, slime molds, and bacteria has long attracted a great deal of attention among biologists, computer animators, and physicists [1–3]. It is crucial to correctly describe the interaction between members of the flock in order to understand and model the flocking behavior. As summarized in [2], a large flock does not have a global leader; instead, the impressive collective flocking phenomena is caused by individual members of the flock following the motion of their neighbors.

In our earlier work [4], we studied the flocking dynamics by using continuum equations for the coarse-grained density field $\rho(\vec{x},t)$ and velocity field $\vec{v}(\vec{x},t)$, written as

$$\partial_t\vec{v} + \lambda(\vec{v}\cdot\nabla)\vec{v} = \alpha\vec{v} - \beta|\vec{v}|^2\vec{v} - \nabla P + D_L\nabla(\nabla\cdot\vec{v}) + D_1\nabla^2\vec{v} + D_2(\vec{v}\cdot\nabla)^2\vec{v} + \vec{f}\,, \quad (1)$$

$$\frac{\partial\rho}{\partial t} + \nabla\cdot(\vec{v}\rho) = 0\,, \quad (2)$$

where β, D_1, D_2, and D_L are all positive, and $\alpha < 0$ in the disordered phase and $\alpha > 0$ in the ordered state. The α and β terms simply make the local $\vec{v}$ have a nonzero magnitude ($= \sqrt{\alpha/\beta}$) in the ordered phase. $D_{L,1,2}$ are diffusion constants. The Gaussian random noise $\vec{f}$ has correlations: $\langle f_i(\vec{r},t)f_j(\vec{r}',t')\rangle = \Delta\delta_{ij}\delta^d(\vec{r}-\vec{r}')\delta(t-t')$ where Δ is a constant, and i, j denote Cartesian components. Finally, the pressure $P = P(\rho) = \sum_{n=1}^{\infty}\sigma_n(\rho-\rho_0)^n$, where ρ_0 is the mean of the local number density $\rho(\vec{r})$ and σ_n are coefficients in the pressure expansion. The final equation (2) reflects conservation of birds.

In [4], we considered the special case of (1) with $\lambda = 1$. Just as the absence of the Galilean invariance for the flock motion allows α and $\beta \neq 0$ in Eq. (1), likewise λ need not be $= 1$. In [5] and this paper, we consider the more generic case $\lambda \neq 1$, which leads to a different direction dependence of the sound speed than when $\lambda = 1$ [6].

In the ordered phase where $\alpha > 0$, the velocity field and the density field can be written as $\vec{v} = v_s\hat{x}_{||} + \vec{\delta v}$, $\rho = \rho_0 + \delta\rho$, where ρ_0 and $v_s\hat{x}_{||}$ are the space averaged density and spontaneous symmetry broken velocity, respectively. The spontaneous symmetry breaking of a vector field leads to large "Goldstone mode" fluctuations; in flocks, this mode is $\vec{v}_\perp$, the projection of $\delta\vec{v}$ perpendicular to $\hat{x}_{||}$ [we will hereafter use "||" ("$\perp$") to denote the projection of any vector along (perpendicular to) $\hat{x}_{||}$]. Indeed, for equilibrium systems, such fluctuations are strong enough in two dimensions to destroy the long range order [7]. One of the remarkable predictions of our continuum model of flocking is that the ordered state is stable even in two dimensions due to the nonequilibrium effect of the nonlinear terms. The mean squared fluctuations in Fourier space in 2D are

$$\langle|\delta\rho(\vec{q},\omega)|^2\rangle = \frac{\Delta q_\perp^2\rho_0^2}{S(\vec{q},\omega)}\,, \quad (3)$$

$$\langle|v_\perp(\vec{q},\omega)|^2\rangle = \frac{\Delta[(\omega - v_sq_{||})^2 + D_\rho q_{||}^4]}{S(\vec{q},\omega)}\,, \quad (4)$$

where the denominator $S(\vec{q},\omega) = [(\omega - v_sq_{||})(\omega - \lambda v_sq_{||}) - c^2q_\perp^2]^2 + [(\omega - v_sq_{||})[D_\perp^R(\vec{q})q_\perp^2 + D_{||}q_{||}^2] - \lambda v_sD_\rho q_{||}^3]^2$. $c = \sqrt{\sigma_1\rho_0}$, $D_\rho = c^2/\alpha$, $D_{||} = D_1 + D_2 + D_\rho$, and $D_\perp^R$, the renormalized diffusion constant, scales as

$$D_\perp^R(\vec{q}_\perp, q_{||};\lambda,\rho_0,\sigma_n) = q_\perp^{z-2}f(q_{||}/q_\perp^\zeta)\,, \quad (5)$$

where the exponents z and ζ are found by RG analysis to be $z = \frac{6}{5}$ and $\zeta = \frac{3}{5}$ for two dimensions, and the scaling function $f(x)$ is universal up to an overall, nonuniversal $\vec{q}$ and ω independent scale factor.

From the above expressions, the correlation functions will have peaks around $\omega_0(\vec{q})$, which satisfies $(\omega_0 - v_sq_{||})(\omega_0 - \lambda v_sq_{||}) - c^2q_\perp^2 = 0$ with solutions: $\omega_0 = \Omega_\pm(\vec{q}) = \frac{1}{2}(1+\lambda)v_sq_{||} \pm [\frac{1}{4}(1-\lambda)^2v_s^2q_{||}^2 + c^2q_\perp^2]^{1/2}$.

This implies that for the wave vector $(q_{||}, q_\perp) = q(\cos(\theta_q), \sin(\theta_q))$ at small q, there should be two peaks in the power spectrum located around $\omega_0 = c_\pm(\theta_q)q$ with the sound speeds:

$$c_\pm(\theta_q) = \tfrac{1}{2}(1 + \lambda)v_s \cos(\theta_q) \pm [\tfrac{1}{4}(1 - \lambda)^2 v_s^2 \cos^2(\theta_q) + c^2 \sin^2(\theta_q)]^{1/2}. \quad (6)$$

The relative strength of the two peaks varies with θ_q. It is not hard to see from Eqs. (3) and (4), that at $\theta_q \sim 0$, $\langle|\delta\rho(\vec{q},\omega)|^2\rangle$ will only have a peak with corresponding wave velocity $c_+(\theta_q = 0) = v_s$, and $\langle|v_\perp(\vec{q},\omega)|^2\rangle$ will only have a peak at $c_-(\theta_q = 0) = \lambda v_s$.

In this paper, we study a discrete model numerically to test the predictions made by our continuum theory. The model we use is very similar to the one studied by Vicsek *et al.* [3]. Following [1], we call our simulated flockers "boids." At a given time t, the position and the direction of the velocity for each boid are given as $(\vec{r}_i(t), \theta_i(t))$ for $i = 1, 2, \ldots, N$. The magnitude of the velocity is fixed: $|\vec{v}_i| = v_0$, its direction is updated at the next time step by averaging over its neighbors' moving directions:

$$\theta_i(t + 1) = \Theta\left(\frac{1}{M}\sum_{j=1}^{M}[\vec{v}_j(t) + \vec{g}_{ij}(t)] + \vec{\eta}_i(t)\right). \quad (7)$$

M is the number of neighbors for boid i within radius R: $r_{ij} = |\vec{r}_i - \vec{r}_j| < R$. The extra interaction term $\vec{g}_{ij} = g_0(\vec{r}_i - \vec{r}_j)[(l_0/r_{ij})^3 - (l_0/r_{ij})^2]$ makes boids repel each other when they are closer than l_0, and attract each other otherwise, with l_0 the average distance between boids in the flock, this interaction will prevent formation of clusters. The noise term $\vec{\eta}_i(t) = \Delta v(\cos[\pi e_i(t)], \sin[\pi e_i(t)])$, where $e_i(t)$ is a random number in the interval $[-1, 1]$. The function $\Theta(\vec{x})$ is just the polar angle of the vector $\vec{x}$. The position update is simply $\vec{r}_i(t + 1) = \vec{r}_i(t) + v_0(\cos[\theta_i(t)], \sin[\theta_i(t)])$. The parameters in this model are R, l_0, Δv, v_0, and g_0.

The particular form of the interactions should not affect the universal predictions of the continuum theory presented above, but rather should change only nonuniversal phenomenological parameters like c, λ, $D_{||}$, etc. They also affect the length scale $l_{\rm NL}$ beyond which the asymptotic long wavelength forms of the correlation functions (3) and (4) apply. Indeed, a one-loop RG analysis predicts $l_{\rm NL} \sim (10 D_\perp^{5/4} D_{||}^{1/4}/\lambda\Delta^{1/2})^{2/(4-d)} O(1)$. Higher loop corrections may affect this result, but it presumably remains accurate to factors of $O(1)$.

For our numerical model, we estimate (on dimensional grounds): $\lambda \sim 1$, $\Delta \sim (\Delta v)^2 \frac{R^d}{t_0}$, $D_{||} \sim D_\perp \sim \frac{R^2}{t_0}$. Inserting these estimates, we find $l_{\rm NL} \sim R(\frac{10R}{\Delta v t_0})^{[2/(4-d)]}$. In our simulation, choosing units of length and time such that $R = t_0 = 1$, and taking $\Delta v \sim \Delta v_c \sim 1/3$ in these units, for $d = 2$ we get the lower bound $l_{\rm NL} > 30$. Previous simulations [8] took $\Delta v \ll 1$, and therefore have a much larger $l_{\rm NL}$. Hence, no nontrivial nonlinear effects could be observed since their systems were much smaller than $l_{\rm NL}$.

The above analysis shows that in order to test the scaling behavior with a reasonable system size, one seeks a small $l_{\rm NL}$ by increasing Δv and decreasing the radius of interaction R as much as possible without entering the disordered phase. In this paper, we report the results of a simulation with system size $L \times L$ with $L = 400$ and the number of boids $N = 320\,000$. We choose $R = 1$, $g_0 = 0.6$, $v_0 = 1.0$, $l_0 = 0.707$. For these parameter values, the flock becomes disordered at $\Delta v_c \sim 0.375$, as shown in Fig. 1(a). The order parameter ϕ is defined simply as the magnitude of the average velocity of the whole flock: $\phi = \frac{1}{N}|\sum_{i=1}^{N} \vec{v}_i|$. To stay in the ordered phase and have enough fluctuations, we choose $\Delta v = 0.15$.

Previous simulations have used periodic boundary conditions [3]. However, for any finite flock, the direction of the average velocity will slowly change, making comparison to the analytical results, which assume infinite system size, and hence a constant direction for $\langle\vec{v}\rangle$, difficult. In order to make $\langle\vec{v}\rangle$ constant in its direction, we impose periodic boundary conditions in one of the directions, say the x direction, and reflecting boundary conditions in the other direction y, i.e., when a boid i with velocity (v_i^x, v_i^y) collides with the "walls" at $y = \pm L/2$, its velocity changes to $(v_i^x, -v_i^y)$. The symmetry broken velocity is thus forced to lie along the x direction, without changing the bulk dynamics of the system. We will hereafter use "||" and x; "$\perp$" and y interchangeably.

We first measure the equal time correlation functions. From Eq. (3), we predict:

$$C_\rho(\vec{q}) = \langle\delta\rho(\vec{q},t)\delta\rho(-\vec{q},t)\rangle = \int\langle|\delta\rho(\vec{q},\omega)|^2\rangle\frac{d\omega}{2\pi} = \frac{2\Delta\rho_0^2 q_\perp^2}{c^2[D_\perp^R(\vec{q})q_\perp^2 + D_{||}q_{||}^2]q^2}\,Y(\theta_q), \quad (8)$$

where $Y(\theta_q)$ is a nonzero $O(1)$ function of θ_q. We see that the equal time correlation function gives us a direct measure of the attenuation. The asymptotic behavior of

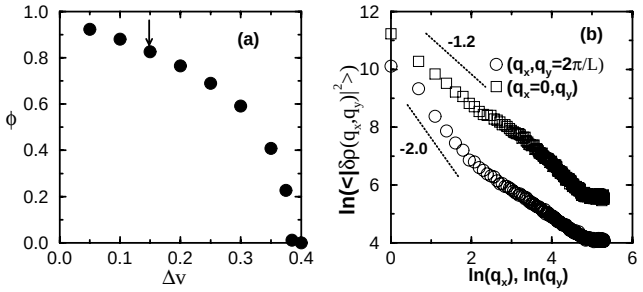

FIG. 1. (a) The order parameter ϕ, as defined in the text, versus the noise strength Δv. The arrow shows the value of Δv at which the fluctuations of the ordered state were calculated. (b) The scaling behavior of the equal time correlation function for the density fluctuations in the two limits as given in Eqs. (9) and (10). The lines illustrate the predicted slopes.

$C_\rho(\vec{q})$ can be expressed as

$$C_\rho(\vec{q}) \sim q_\perp^{-z}, \qquad q_\perp \gg q_\parallel, \tag{9}$$

$$\sim q_\parallel^{-2}, \qquad q_\parallel \gg q_\perp \gg q_\parallel^{1/\zeta}. \tag{10}$$

In Fig. 1(b), we have plotted the equal time density correlation functions in Fourier space: $C_\rho(q_\parallel, q_\perp = 2\pi/L)$ versus $q_\parallel$ and $C_\rho(q_\parallel = 0, q_\perp)$ versus $q_\perp$ from our simulation. The scaling behavior at long length scales can be fitted with $C_\rho(q_\parallel, q_\perp = 2\pi/L) \sim q_\parallel^{-2.05}$ and $C_\rho(q_\parallel = 0, q_\perp) \sim q_\perp^{-1.23}$. These two exponents show excellent agreement with the analytical results -2 and $-\frac{6}{5}$, respectively. As can be seen from Fig. 1(b), the scaling region for the current simulation covers slightly less than one decade in $q_\perp$. It is not surprising that earlier simulations of smaller systems with less carefully chosen parameters (leading to larger $l_{\rm NL}$), did not observe the nontrivial scaling.

Another interesting measurement of the simulation is the anomalous diffusion of individual boids in the direction y perpendicular to the flock's moving direction. We measure the "width" of the dispersion of an ensemble of boids: $w^2(t) = \langle [\, y_i(t) - y_i(0)]^2 \rangle$. The analytical behavior of the anomalous diffusion can be obtained from $w^2(t) \sim \int_0^t \int_0^t \langle v_y^i(t') v_y^i(t'') \rangle dt'\, dt''$ where $v_y^i(t)$ is the velocity of the ith boid along the y direction at time t. The velocity correlation function is given by (4)

$$\langle v_y^i(0) v_y^i(t) \rangle \sim \langle v_y(\vec{x} + \phi \hat{x} t, t) v_y(\vec{x}, 0) \rangle = \int \frac{\exp[i(\omega - \phi q_\parallel)t] \Delta(\omega - v_s q_\parallel)^2 d^2q\, d\omega}{S(\vec{q}, \omega)} \sim t^{1-1/\zeta}, \tag{11}$$

which implies $w^2(t) \sim t^{3-1/\zeta} = t^{4/3}$. In Fig. 2(b), we have plotted the width squared $w^2(t)$ versus time t in log-log scale. The scaling can be fitted nicely with $w^2(t) \sim t^{1.3}$, which agrees well with the analytical result $t^{4/3}$. We have also simulated Vicsek's original model, but with parameters Δv, etc., chosen to make $l_{\rm NL}$ as small as possible, and found again $w^2(t) \sim t^{1.3}$. This supports the universality of our analytic results.

Besides the scaling behavior, the analytical results (3), (4) also imply the existence of sound waves as reflected in the peaks of the correlation functions, Eqs. (3) and (4). From Eq. (3), at a given value of $\vec{q}$, the correlation function has peaks at $\omega = c_\pm(\theta_q) q$. We have measured the power spectrum in the y direction: $\langle |\delta\rho(q_\parallel = 0, q_\perp = \frac{2\pi}{L} n_\perp, \omega = \frac{2\pi}{T} n_\omega)|^2 \rangle$ ($T = 1024$) with different values of $n_\perp (= 1, 2, \ldots, 20)$. Figure 3 shows the power spectra for $n_\perp = 5, 10, 20$. The spectra are symmetric around $\omega = 0$ (we show only half of the spectrum for $\omega > 0$) and the positions of the peaks n_ω^* versus n_y are shown in the inset of Fig. 3, whose slope determines the sound velocity in the y direction $c = 0.62$. We have calculated the power spectrum of $v_\perp$ in the y direction, which shows the same peaks.

An interesting phenomenon happens when we calculate the spectrum along the x direction, i.e., with $q_\parallel \neq 0$ and $q_\perp = 0$. As predicted by Eqs. (3) and (4), we see one single peak for each correlation function. Indeed, as shown in Fig. 4, each power spectrum shows only one peak, and again as predicted by (3) and (4), the peak for the $v_\perp$ power spectrum is at a different ω than the peak of the density power spectrum. This means that the velocity fluctuations propagate with a different velocity than the density fluctuations in the x direction.

We can then extract from Fig. 4 the values of $v_s = 0.93$, $\lambda = 0.75$. (The fact that $\lambda \neq 1$ reflects the absence of Galilean invariance.) With the value of $c = 0.62$ determined through Fig. 3, we can predict the sound speeds in all other directions of propagation from Eq. (6) with no adjustable parameters. To test these predictions, we have also calculated the power spectra for the density and the velocity fields at two other angles: $\tan(\theta_q) = 1/3, 4$. For the

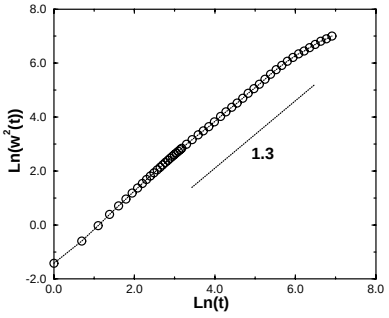

FIG. 2. The log-log plot of the anomalous transverse diffusion of an individual boid versus time.

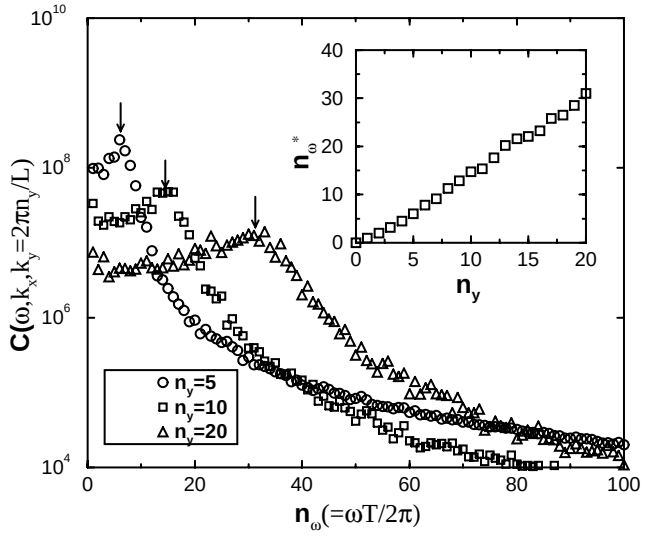

FIG. 3. The power spectrum of the density for different wave vectors. The inset shows the peak positions of the power spectrum versus wave number. The linear slope determines the sound velocity.

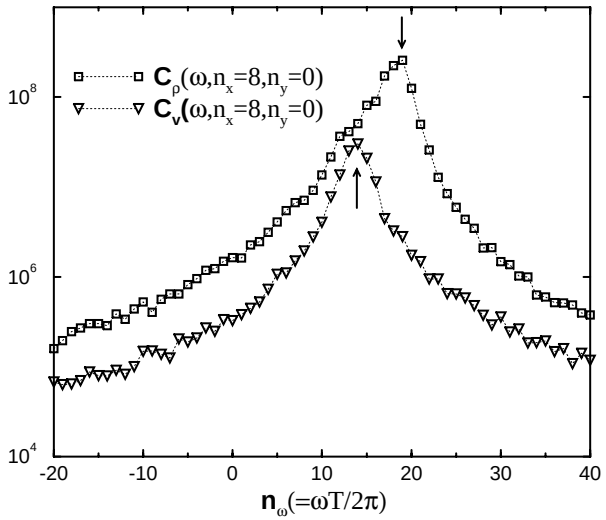

FIG. 4. Power spectra for the density and velocity fluctuations for the same wave vector along the parallel direction. The peaks of the two curves are clearly different.

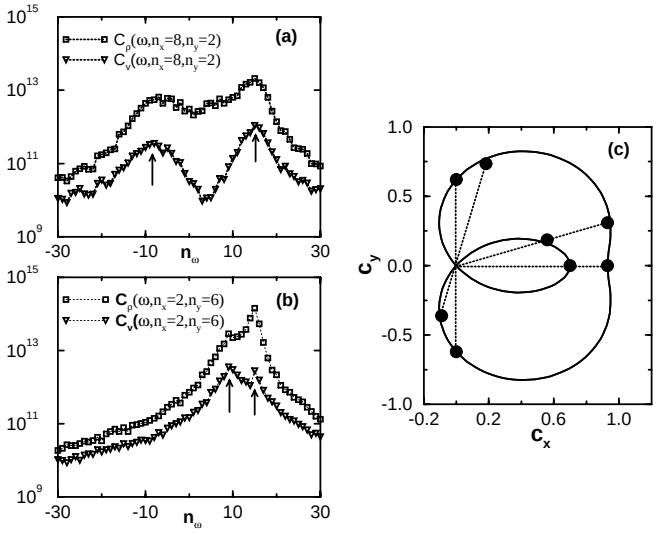

FIG. 5. The power spectra for the density and the velocity fluctuations in directions (a) $\theta_{q,1} = \arctan(4)$ and (b) $\theta_{q,2} = \arctan(1/3)$. The two peaks are clearly visible, albeit with different magnitudes. In (c), the wave velocities $c_\pm(\theta_q)$ are plotted in polar angle coordinates $(c_\pm(\theta_q), \theta_q)$ for the four different directions $\theta_q = 0, \theta_{q,1}, \theta_{q,2}, \pi/2$, the two axes represent $c_x = c_\pm(\theta_q)\cos(\theta_q)$ and $c_y = c_\pm(\theta_q)\sin(\theta_q)$ respectively. The solid curve is the prediction from Eq. (6) in the text.

large angle $\theta_{q,1} = \arctan(4) = 76.0°$, the data are shown in Fig. 5(a). The peaks for ρ and $v_\perp$ are at the same location, and the wave velocities are $c_\pm(\theta_{q,1}) = 0.75, -0.37$. The data for $\theta_{q,2} = \arctan(1/3) = 18.4°$ are shown in Fig. 5(b). The peak at $\omega = c_-(\theta_{q,2})$ is just barely visible in the density correlation, but both peaks show very well in the velocity correlation, and the peaks for both correlation functions are at the same locations, giving the velocity $c_\pm(\theta_{q,2}) = 0.97, 0.59$. In Fig. 5(c), we have plotted the angle dependence of the wave velocity as predicted in Eq. (6) in polar angle coordinates $[c_\pm(\theta_q), \theta_q]$, with the values of v_s, λ, and c determined earlier. We have included in Fig. 5(c), the sound velocities for the two angles $\theta_{q,1}$ and $\theta_{q,2}$. The agreement with the predicted velocities is excellent.

In summary, the numerical simulations reported here strongly support our analytical continuum theory of flocks. The observed sound speeds agree very well with our predictions. In particular, our analytical model's assertion that Galilean invariance is absent is confirmed by the existence of two different nonzero sound speeds for propagation along the mean direction of flock motion. In addition, the sound attenuation shows the anomalous scaling we predict [9].

Y. Tu is grateful to Dr. R. Walkup for helping with the parallel programming for this problem on an IBM SP-1 parallel computer. J. Toner thanks the Aspen Center for Physics and the Center for Chaos and Complexity at the University of Colorado, Boulder for their hospitality while a portion of this work was completed.

[1] C. Reynolds, Comput. Graph. **21**, 25 (1987); J. L Deneubourg and S. Goss, Ethol. Ecol. Evolution **1**, 295 (1989); A. Huth and C. Wissel, in *Biological Motion*, edited by W. Alt and E. Hoffmann (Springer-Verlag, New York, 1990), pp. 577–590. We thank D. Rokhsar for calling these. references to our attention.
[2] B. L. Partridge, Sci. Am. **246**, No. 6, 114–123 (1982).
[3] T. Vicsek *et al.*, Phys. Rev. Lett. **75**, 1226 (1995).
[4] J. Toner and Y. Tu, Phys. Rev. Lett. **75**, 4326 (1995).
[5] J. Toner and Y. Tu (to be published).
[6] Additional nonlinear terms $\lambda_2\vec{v}(\nabla\cdot\vec{v})$ and $\lambda_3\nabla(|\vec{v}|^2)$ are also allowed, but do not change any results in the broken symmetry state in $d = 2$.
[7] N. D. Mermin and H. Wagner, Phys. Rev. Lett. **17**, 1133 (1966).
[8] A. Czirok, H. E. Stanley, and T. Vicsek, J. Phys. A **30**, 1375 (1997).
[9] Our original derivation of the scaling exponents z, ζ and χ in Ref. [4] assumed $\lambda = 1$, which it need not be in general. However, we have shown in Ref. [5] that the exponents are unchanged for a finite range of λ's.